HHS Public Access

Author manuscript

Matrix Biol. Author manuscript; available in PMC 2018 December 01.

Published in final edited form as:

Matrix Biol. 2017 December ; 64: 81–93. doi:10.1016/j.matbio.2017.08.004.

Decorin and Biglycan Are Necessary for Maintaining Collagen Fibril Structure, Fiber Realignment, and Mechanical Properties of Mature Tendons

Kelsey A. Robinson[a], **Mei Sun**[b], **Carrie E. Barnum**[a], **Stephanie N. Weiss**[a], **Julianne Huegel**[a], **Snehal S. Shetye**[a], **Linda Lin**[b], **Daniel Saez**[b], **Sheila M. Adams**[b], **Renato V. Iozzo**[c], **Louis J. Soslowsky**[a], and **David E. Birk**[b]

[a]McKay Orthopaedic Research Laboratory, University of Pennsylvania, 424 Stemmler Hall, 36th and Hamilton Walk, Philadelphia, PA, 19104-6081

[b]Department of Molecular Pharmacology & Physiology, Morsani College of Medicine, University of South Florida, Tampa, FL 33612

[c]Department of Pathology, Anatomy and Cell Biology, Sidney Kimmel Medical College, Thomas Jefferson University, Philadelphia, PA 10107

Abstract

The small leucine-rich proteoglycans (SLRPs), decorin and biglycan, are key regulators of collagen fibril and matrix assembly. The goal of this work was to elucidate the roles of decorin and biglycan in tendon homeostasis. Our central hypothesis is that decorin and biglycan expression in the mature tendon would be critical for the maintenance of the structural and mechanical properties of healthy tendons. Defining the function(s) of these SLRPs in tendon homeostasis requires that effects in the mature tendon be isolated from their influence on development. Thus, we generated an inducible knockout mouse model that permits genetic ablation of decorin and biglycan expression in the mature tendon, while maintaining normal expression during development. Decorin and biglycan expression were knocked out in the mature patellar tendon with the subsequent turnover of endogenous SLRPs deposited prior to induction. The acute absence of SLRP expression was associated with changes in fibril structure with a general shift to larger diameter fibrils in the compound knockout tendons, together with fibril diameter heterogeneity. In addition, tendon mechanical properties were altered. Compared to wild-type controls, acute ablation of both genes resulted in failure of the tendon at lower loads, decreased stiffness, a trend toward decreased dynamic modulus, as well as a significant increase in percent relaxation and tissue viscosity. Collagen fiber realignment was also increased with a delayed and slower in response to load in the absence of expression. These structural and functional changes in response to an acute loss of decorin and biglycan expression in the mature tendon demonstrate a significant role for these SLRPs in adult tendon homeostasis.

Correspondence to: David E. Birk, Ph.D., Department of Molecular Pharmacology & Physiology, MDC08, Morsani College of Medicine, University of South Florida, Tampa, FL 33612, *Tel: 813-974-8598*, dbirk@health.usf.edu.

Keywords

Tendon; Decorin; Biglycan; Collagen fibril; Fiber realignment; Structure; Mechanical properties; Conditional knockout mice

Introduction

Tendons are dense connective tissues that transmit force from muscle to bone. Tendons are composed of tenocytes within a highly organized collagen network linked by small leucine rich proteoglycans (SLRPs) [1, 2]. Collagen I is the most abundant component of tendons and is assembled into collagen fibrils. Collagen fibrils are organized into fibers providing tensile strength. The fibrils and highly organized bundles of collagen fibers interact with SLRPs in the extracellular matrix. Tendons express decorin and biglycan (class I) [3, 4], as well as fibromodulin and lumican (class II) [5] SLRPs, and both classes have been implicated in the regulation of collagen fibrillogenesis [5–10]. SLRPs consist of a protein core characterized by leucine-rich repeats composing a central domain flanked by N- and C-terminal cysteine-rich domains [10–12]. The most abundant SLRPs in tendon are decorin and biglycan, with one or two dermatan/chondroitin sulfate glycosaminoglycan chains (GAG), respectively. Both decorin and biglycan share a common binding site for collagen I with decorin binding to collagen I with a greater affinity than biglycan [13–15]. During tendon development, decorin expression peaks when collagen fibrils are undergoing lateral growth and continues to be expressed during maturation and aging [1, 16], which suggests a role in the maintenance of collagen homeostasis. In contrast, biglycan expression peaks during post-natal development and then rapidly declines [1].

SLRPs impact the hierarchical organization of tendon and its mechanical properties, but these structure-function relationships are not well understood. Tendons from decorin knockout mice have decreased viscoelastic properties including larger and faster stress relaxation [17], decreased strain rate sensitivity [18], but no change in elastic properties [19]. Biglycan-null tendons demonstrated less alteration in mechanical properties than the decorin-null mice, however, tensile dynamic modulus was increased when expression was reduced [20]. Structurally, decorin deficiency manifests with irregularly contoured large diameter collagen fibrils [21] and biglycan-null [22] tendons have an increased range of collagen fibril diameter and irregular profile in mouse tendon and smaller average fibril diameter [8]. Interestingly, in the absence of decorin, biglycan is overexpressed and its binding to collagen I functionally compensates for decorin [3, 23]. Clinically, up-regulation of biglycan has been noted in patients with reduced decorin expression [24]. In addition to the tendon, several studies suggest functional compensation for decorin by biglycan in single null models. For example, the posterior frontal suture of the developing calvaria fuses normally in the absence of either decorin or biglycan, but fails to fuse in mice null for both SLRPs [25]. Mice that lack both decorin and biglycan exhibit a collagen fibril morphology that is significantly more abnormal than either single deficiency, which supports the hypothesis that they have overlapping functions that permit functional compensation in single null mice [8, 23]. Given the apparent overlap in the functions of decorin and biglycan during development, it is unclear whether the changes in collagen organization and

mechanical properties in decorin null models are due to the absence of decorin, over expression of biglycan, or some combination of the two. Knockout of both decorin and biglycan expression in mature tendons would permit the study of the decorin phenotype in the absence of functional compensation by biglycan.

The absence of decorin or biglycan during development produces a mature tendon that is structurally different from wild type tendon [3, 7, 8, 19, 26]. However, elucidation of the function of SLRPs in tendon homeostasis requires that effects in the mature tendon be distinguished from their influence on development. In this study, we generated an inducible knockout mouse model that allows, for the first time, the investigation of the post-developmental functions of these two key SLRPs in tendon homeostasis. Our overall objective was to define the roles of decorin and biglycan expression in tendon homeostasis. We hypothesize that the acute loss of decorin and biglycan expression in the mature tendon will have detrimental effects on the structural and mechanical properties of healthy tendons. In addition, decorin has been proposed to have a dominant role and biglycan a modulatory role in the regulation of tendon matrix assembly [10], and knockout of decorin can result in an up-regulation of biglycan with functional compensation [3, 23]. Therefore, dual genetic ablation *Dcn* and *Bgn* genes will reflect a decorin-null phenotype without compensatory up-regulation of biglycan, thereby defining the regulatory role of decorin in tendon homeostasis.

Results

Characterization of Inducible Knockout Model

To analyze the roles of decorin and biglycan expression in maintaining structure and function in mature tendons, a Tamoxifen (TM)-inducible compound-null mouse model was generated. Conditional decorin-null ($Dcn^{flox/flox}$) and biglycan-null ($Bgn^{flox/flox}$) mouse models were cross bred to produce a compound decorin- and biglycan-null mice ($Dcn^{flox/flox}/Bgn^{flox/flox}$). The strategy for producing the conditional *Dcn* and *Bgn* mouse models is presented in Supplemental Figs. S1 and S2. In these conditional models loxP elements flank exon 3 in *Dcn* and exon 4 in *Bgn*. The conditional *Dcn* and *Bgn* mice with these floxed alleles (Supplemental Fig. S3A) were cross-bred with knockin ubiquitous TM-inducible Cre (Cre/ERT2) mice which generated stable bitransgenic TM-inducible decorin- and biglycan-null mouse models (Supplemental Fig. S3A). Induction with Tamoxifen resulted in excision of the floxed exons (Supplemental Fig. S3B). Decorin and biglycan expression and content were analyzed in immature (day 45) flexor digitorum longus (FDL) tendons 24 days after induction of the knockout. This resulted in a knockdown of *Dcn* and *Bgn* expression to basal levels (Supplemental Fig. S4A,B). As expected, this knockout of *Dcn* and *Bgn* expression was associated with a significant reduction of decorin or biglycan protein core (Supplemental Fig. S4C,D). The remaining Dcn and Bgn protein core, observed 24 days after induction of the knockout, is consistent with an incomplete turnover of endogenous decorin and biglycan deposited into the tendon extracellular matrix prior to induction of the null genotype.

Gene and Protein Expression in Patellar Tendon

In the mature patellar tendon of this TM-inducible compound-null mouse model (I-*Dcn*$^{-/-}$/*Bgn*$^{-/-}$), induction of Cre excision after TM administration resulted in a knockout of both decorin and biglycan expression (Fig. 1A,B). Thirty days after Cre induction, both decorin and biglycan expression were at baseline in the day 150 patellar tendons. The baseline was comparable to that observed in the well-characterized traditional decorin and biglycan knockout mice [21, 22]. There was a significant reduction in immunofluorescence reactivity for both decorin and biglycan at day 150 (Fig. 1C,D), however, more reactivity was present than observed in the traditional knockout models used as a negative control. The small amount of residual reactivity in the I-*Dcn*$^{-/-}$/*Bgn*$^{-/-}$ tendons 30 days after induction of the knockout compared with non-induced control mice is consistent with incomplete turnover of the SLRPs deposited pre-induction.

Phenotype, Tendon Cellularity, and Cell Shape

Wild type and I-*Dcn*$^{-/-}$/*Bgn*$^{-/-}$ mice were similar in appearance without gross differences in tendon length or morphology. At the time of induction (day 120), there was a trend towards decreased weight in I-*Dcn*$^{-/-}$/*Bgn*$^{-/-}$ mice compared to wild type controls (WT: 23.63g ± 1.26g, I-*Dcn*$^{-/-}$/*Bgn*$^{-/-}$: 22.69g ± 1.62g, p = 0.07). At the time of sacrifice (day 150), I-*Dcn*$^{-/-}$/*Bgn*$^{-/-}$ mice weighed significantly less than wild type controls (WT: 24.6g ± 1.35g, *Dcn*$^{-/-}$/*Bgn*$^{-/-}$: 23.63g ± 1.26g, p = 0.04). There were no significant differences in the change in weight from the time of injection to sacrifice (WT: 1.00g ± 1.36g, *Dcn*$^{-/-}$/*Bgn*$^{-/-}$: 0.94g ± 1.57g, p = 0.9) (Supplemental Fig. S5A,B). Knockout of both decorin and biglycan expression had no effect on cell density or cell shape in mature patellar tendons thirty days after gene excision as determined histologically (Supplemental Fig. S5C).

Fibril Structure

The structural properties of tendon collagen fibrils were analyzed in mature (day 150) I-*Dcn*$^{-/-}$/*Bgn*$^{-/-}$ patellar tendons 30 days after TM-induced knockout of *Dcn* and *Bgn* expression, and compared to wild type control mice. Mature tendon collagen fibrils 30 days after the knockout of both decorin and biglycan expression had structures comparable to the wild type controls with circular cross-sectional profiles. However, fibrils from I-*Dcn*$^{-/-}$/*Bgn*$^{-/-}$ tendons had larger diameters than those in the wild type tendons (Fig. 2A–D). The I-*Dcn*$^{-/-}$/*Bgn*$^{-/-}$ median fibril diameter was increased compared to the wild type controls (110.5 nm versus 98.4nm). In addition, there was a broader range of diameters in the I-*Dcn*$^{-/-}$/*Bgn*$^{-/-}$ tendons with interquartile ranges (Q3-Q1) of 80.5nm compared with a wild type range of 70.2nm. There was a conspicuous right hand shoulder with markedly larger diameter fibrils in the I-*Dcn*$^{-/-}$/*Bgn*$^{-/-}$ mice compared to wild type controls. The increase in the interquartile range (Q3-Q1) is indicative of increased diameter heterogeneity in knockout tendons. Overall, differences in the fibril distribution median, interquartile range, and large diameter outliers were observed between the two groups (Fig. 2E). Fibril density also was analyzed after knockout of decorin and biglycan expression for 30 days in the mature tendon. The fibril density was significantly lower ($p<0.005$) in I-*Dcn*$^{-/-}$/*Bgn*$^{-/-}$ tendons compared with the wild type controls, the means ± sd (n) were 79.9 ± 11.6 (55) fibrils/μm^2 versus 92.2 ± 14.3 (42) fibrils/μm^2, respectively (Fig. 2F).

Biomechanical Properties

The impact of decorin and biglycan expression on function in mature tendons was determined. The mechanical properties of mature tendons 30 days after knockout of decorin and biglycan expression in I-*Dcn*$^{-/-}$/*Bgn*$^{-/-}$ mice were compared to wild type tendons. There were no differences in tendon cross-sectional area of I-*Dcn*$^{-/-}$/*Bgn*$^{-/-}$ mice compared to wild types (data not shown). The I-*Dcn*$^{-/-}$/*Bgn*$^{-/-}$ tendons failed at lower loads than wild type tendons when subjected to a tensile ramp to failure test (Fig. 3A). This test produces a stress-strain curve with “toe” and “linear” regions that can be approximated by a bilinear fit. The toe and linear moduli, which are the slopes of these regions of the curve, serve as a measure of stiffness. The transition between these two regions represents the strain at which the continued application of stress more rapidly induces strain. I-*Dcn*$^{-/-}$/*Bgn*$^{-/-}$ tendons undergo this transition later than wild type tendons (Fig. 3B).

Tendons exhibit properties of viscous and elastic materials when deformed, which results in their response to a load changing over time. Specifically, the stress in the tendon decreases when it is held at a constant strain, a property unique to viscoelastic materials known as “stress-relaxation”. Differences in tissue viscoelasticity in the I-*Dcn*$^{-/-}$/*Bgn*$^{-/-}$ tendons were observed compared with wild type control tendons. When held at 5% strain, compound knockout tendons demonstrated an increased percent relaxation compared to wild type tendons (Fig. 4A). The midsubstance of I-*Dcn*$^{-/-}$/*Bgn*$^{-/-}$ tendons exhibited decreased stiffness in the linear region of the test (Fig. 4B). There were no regional differences in linear modulus (Fig. 4C). Compound knockout tendons exhibited significantly increased tan(δ), a measure of tissue viscoelasticity defined as the ratio of dissipated to stored force during cyclic loading, at all frequencies and strains tested (Fig. 5). In addition, there was a trend towards decreased dynamic modulus (Fig. 5). Dynamic modulus is defined as the ratio of induced stress to applied strain during cyclic loading and is a measure of the tendon’s ability to transfer force to bone during loading. A decreased dynamic modulus signifies that the tendon produces less stress for the applied strain.

Collagen fiber realignment in response to load was altered in mature I-*Dcn*$^{-/-}$/*Bgn*$^{-/-}$ tendons with an induced knockout of both decorin and biglycan expression. Circular variance is a measure of collagen fiber alignment during loading and a reduction in circular variance is indicative of increased fiber alignment. The ratio between the circular variance at a given strain to the circular variance at zero strain was used to compare the collagen realignment in each group during the ramp to failure. I-*Dcn*$^{-/-}$/*Bgn*$^{-/-}$ tendons underwent more realignment than wild types in the linear region of the test (Fig. 6). In addition, wild type tendons realigned earlier and more rapidly than compound knockouts at the tendon midsubstance (between 0 and 3% strain compared to between 1 and 7% strain) (Fig. 7).

Discussion

The objective of this study was to define the roles of decorin and biglycan in tendon homeostasis. Acute loss of decorin and biglycan expression in the mature tendon had detrimental effects on the structural and mechanical properties of the tendons. A tamoxifen-inducible compound decorin and biglycan knockout mouse model was developed, allowing for temporal specificity of the knockout. Previous analyses of decorin-null and biglycan-null

mouse models demonstrate that both decorin and biglycan have a key role(s) in the development of tendons, regulating growth and assembly of collagen fibrils [1, 3, 4, 27]. Therefore, the ability to knockout expression of these genes at maturity allows their roles in tendon homeostasis to be isolated from their developmental effects.

This study successfully developed and characterized a novel compound inducible knockout model that permitted investigation of the roles of both decorin and biglycan in tendons that underwent normal development. There was an absence of gross changes in the mice as well as no histological changes in the I-*Dcn*$^{-/-}$/*Bgn*$^{-/-}$ tendons. The lack of gross changes at these levels minimizes the potential for secondary effects such as those due to abnormal development that are important in the interpretation of musculoskeletal studies. In addition, the creation of this model permits the use of inducible single knockout models of decorin or biglycan in future studies. This will be critical to defining the dominant and modulatory regulatory roles of these SLRPs in tendons and other tissues.

The I-*Dcn*$^{-/-}$/*Bgn*$^{-/-}$ mice were null with respect to expression of both SLRPs 30 days post induction in the mature patellar tendons (day 150). Our supplemental data and unpublished work demonstrate virtually complete Cre excision 5 days post induction with loss of expression of both decorin and biglycan. These data support a lack of both expression and new SLRP synthesis and deposition into the tendon matrix during the 30-day period in our studies. The use of a ubiquitous Cre also excludes translation and secretion at other sites. There is evidence that SLRPs from other sites can be deposited into remote tissues, particularly during inflammatory responses [28, 29]. Also, systemically administered SLRPs can be integrated into tissues [30]. Use of a ubiquitous inducible knockout in the current model precludes secondary effects resulting from the systemic translocation and deposition of decorin and/or biglycan into the tendon matrix. Future work will address the roles of SLRPs in the injury response. While the day 150 I-*Dcn*$^{-/-}$/*Bgn*$^{-/-}$ patellar tendons were null for expression, there was reactivity for residual decorin and biglycan. There was a significant decrease in the reactivity compared to wild type controls 30 days post-induction. However, while not analyzed in the current work, there was a presumed graded decrease across the 30-day period and the functions of the endogenous SLRPs must be considered. Future analysis of less acute periods will address this issue. However, these studies clearly demonstrate structural and functional differences in the I-*Dcn*$^{-/-}$/*Bgn*$^{-/-}$ compared to wild type controls even with retention of some endogenous decorin and biglycan.

The I-*Dcn*$^{-/-}$/*Bgn*$^{-/-}$ tendons had altered structure at the fibril level. Interestingly, there was an increase in large diameter collagen fibrils within 30 days of SLRP removal from mature I-*Dcn*$^{-/-}$/*Bgn*$^{-/-}$ patellar tendons. A general increase in fibril diameters and a shift in the diameter distribution to larger diameters compared to control tendons was observed. Traditional compound decorin- and biglycan-null tendons exhibit collagen fibril structures that are significantly more abnormal than what is observed here after acute knockout of expression [8]. In traditional decorin-null tail tendons there was an increased average fibril diameter due to a population of unusually large fibrils compared to wild types [3, 8]. This is similar to what is seen here in compound knockouts that underwent normal development, supporting the notion that this conditional compound knockout model may actually reflect the decorin-null phenotype. Biglycan expression normally decreases after development is

complete [3]; therefore, decorin may be the primary regulator of tendon homeostasis at maturity. The severe phenotype seen in conventional compound decorin and biglycan knockout mice [8] may ultimately be due to absent biglycan expression during development and absent functional compensation for decorin at maturity. Both decorin and biglycan regulate lateral growth of collagen fibrils during development [3, 10]. After acute knockout of both decorin and biglycan expression the fibril structural data are consistent with a dysfunctional regulation resulting in continued lateral growth and a shift towards larger diameter collagen fibrils.

These structural changes were associated with an inferior response during dynamic loading in tendons 30 days after inactivation of the genes. Compared to wild type controls, knockout of expression resulted in a failure at lower loads, decreased stiffness, and a trend toward decreased dynamic modulus as well as an increase in percent relaxation, and tissue viscosity within thirty days. Collagen fiber realignment was increased, and the process was delayed and occurred more slowly in response to load in the absence of expression. To our knowledge, these parameters have not been analyzed in traditional compound decorin- and biglycan-null models where expression was absent from conception. However, an analysis of decorin-null [16] and biglycan-null [20] tendons suggest that the inferior mechanical properties after acute knockout of both decorin and biglycan expression were substantially less than that expected based on additive effects observed in traditional decorin and biglycan knockout tendons [16, 20].

The data support a relationship between altered structural properties and altered functional properties after the acute knockout of decorin and biglycan. The altered fibril diameters and fibril density would directly impact the mechanical properties. There also was increased heterogeneity in fibril diameter and density leading to an overall less uniform composition that may have functional implications. In addition, the interfibrillar interactions mediated by decorin and biglycan were absent which would be expected to impact the functional properties of higher order structures, fibers. Decorin and biglycan crosslink collagen fibrils and may participate in force transfer between fibrils [31]. It can be argued that they help to maintain the mechanical integrity of the tissue and their removal may result in more fibril sliding and deformation, leading to increased baseline realignment, decreased failure load, and altered mechanics. The loss of these crosslinking interactions would result in increased dissipation of energy during cyclic loading because the proteoglycans that help to maintain the mechanical integrity to resist fibril sliding are absent. Finally, decreased tendon hydration due to decreased SLRP/GAG content also would be expected. Since GAG content affects the viscoelastic behavior of tendon a loss of SLRPs would reduce the mechanical integrity of the fibers and would contribute to the deterioration of mechanical properties.

While this is the first study to characterize the mechanical properties of tendons null for both decorin and biglycan, it is interesting to note that the reduced failure loads seen here were similar to those of decorin-null and compound decorin and biglycan-null uteri [32]. Mature decorin-null tendons also have been noted to have decreased maximum load, stiffness, and modulus [3]. These changes appear to be occurring in our conditional I-$Dcn^{-/-}/Bgn^{-/-}$ tendons, as evidenced by decreased failure load, excessive dissipation of energy during dynamic loading, a trend towards loss of dynamic modulus, and decreased midsubstance

stiffness compared to wild type tendons. The changes in these mechanical parameters suggest that after development, decorin is a more critical regulator of mechanical properties, specifically for tissues that undergo tensile loading, than biglycan.

Compared to wild type tendons, I-*Dcn*$^{-/-}$/*Bgn*$^{-/-}$ tendons also responded to load with increased collagen fiber realignment at strains corresponding to the linear region of the test, which may be due to increased fibril deformation [33] or decreased collagen cross-linking, although the precise effects of cross-linking on mechanical properties are not well established [34]. They also realign later than wild types and over a wider range of strains, which supports the notion that decorin and biglycan are involved in the maintenance of the normal tendon load response after development. Interestingly, mature decorin-null tendons do not realign differently than wild type tendons [16], therefore, the increased realignment seen in I-*Dcn*$^{-/-}$/*Bgn*$^{-/-}$ tendons suggests that biglycan expression may compensate for these changes at maturity. The rapid rate at which these changes occurred suggests that decorin plays a critical role in maintaining tendon structure and function. These tendons appear and behave like decorin-null tendons, which supports the role of decorin as a key regulator of tendon structure and function after development. Inhibition of compensatory biglycan expression in decorin-null tendons may permit changes in collagen fiber ultrastructure which lead to the decreased strength and changes in realignment seen in compound knockouts.

This novel inducible I-*Dcn*$^{-/-}$/*Bgn*$^{-/-}$ model successfully permitted the analysis of the roles of decorin and biglycan in tendon homeostasis by removing the variable of SLRP expression during development. This permitted the demonstration that these fibril-associated proteoglycans have substantial roles in determining/altering tendon structure and function in mature tissues. However, further study of decorin and biglycan independently would provide information defining the specific roles these proteins play at maturity. We have suggested that decorin has a dominant role while biglycan has modulatory regulatory roles [10]. Further analysis of the single-null models would clarify their specific roles. This work begins to define the importance of decorin and biglycan in maintaining normal physiology in the mature tendon. The acute loss of both decorin and biglycan expression in the mature *Dcn*$^{-/-}$/*Bgn*$^{-/-}$ tendon demonstrates a significant role for these SLRPs in tendon homeostasis. An understanding of these structure-function relationships will help elucidate the pathophysiology underlying tendon injuries and may ultimately help direct future treatment strategies. Future work will consider the role of decorin and biglycan independently, as well as their impact on the mechanical and structural properties of aged tendons.

Experimental procedures

This study was approved by the University of South Florida and the University of Pennsylvania Institutional Animal Care and Use Committees. These studies were performed using female wild type mice (C57/BL6 Charles River) and our tamoxifen (TM) inducible compound decorin/biglycan knockout mouse model (TM- *Dcn*$^{-/-}$/*Bgn*$^{-/-}$) in a C57/BL6 Charles River background.

Development of decorin and biglycan conditional mouse models

A stable bitransgenic tamoxifen inducible compound decorin/biglycan-null (I-*Dcn*$^{-/-}$/*Bgn*$^{-/-}$) mouse model was created for use in these studies. We obtained the *Dcn* (IKMC project: 71880) and *Bgn* (IKMC project: 45577) targeting vectors from EUCOMM. Both vectors produce a knockout-first-reporter tagged insertion with subsequent excision of the FRT flanked sequence yielding the *Dcn*$^{flox/flox}$ or *Bgn*$^{flox/flox}$ conditional alleles. Briefly, the targeting vectors include exon 3 for *Dcn* and exon 4 for *Bgn* flanked by loxP elements, a neo cassette and LacZ reporter sequence flanked by FRT sequences and a PGK/DTA cassette for negative selection. The strategy for decorin and biglycan is presented in Supplemental Figs. S1A and S2A, respectively. Targeted ES cells for *Dcn* or *Bgn* in JM8A3.N1 C57/6n agouti converted male mouse ES cells were selected and characterized using PCR and Southern analyses (Supplemental Figs. S1B and S2B). Karyotype analysis was performed and appropriate targeted ES cell clones for *Dcn* and *Bgn* were injected into wild type mouse blastocysts. Chimeric mice derived from the *Dcn* (4 mice, 10–70% chimeric) and *Bgn* (4 mice, 5–80% chimeric) clones were obtained. Chimeric males were crossed with C57 BL/6 Charles River females to create targeted *Dcn*$^{ta/wt}$ *or Bgn*$^{ta/wt}$ mice. As previously described [35], these targeted mice were crossed with a germline-specific FLPe transgenic mouse (B6;SJL-Tg(ACTFLPe)9205Dym/J, Jackson Labs) to remove the FRT flanked neo cassette and Lac Z sequences which yielded the heterozygous floxed *Dcn*$^{flox/wt}$ *or Bgn*$^{flox/wt}$ mice. These mice were bred to homozygosity, generating conditional *Dcn*$^{flox/flox}$ and *Bgn*$^{flox/flox}$ mice and the compound targeted mice were created by cross breeding. The bitransgenic TM-inducible mouse models were generated by breeding the conditional *Dcn*$^{flox/flox}$ *and Bgn*$^{flox/flox}$ mice with mice expressing a TM-inducible Cre (Supplemental Fig. S3A). Knockin TM-inducible Cre mice (B6.129-Gt(ROSA)26Sortm1(cre/ERT2)Tyj/J, Jackson Labs) were used to generate the bitransgenic inducible models. Efficient Cre excision was obtained after induction with TM (Supplemental Fig. 3B).

To determine the optimum TM dose needed for Cre excision, male inducible Cre mice were bred with mT/mG reporter mice (Jackson Labs). TM base (T5648, Sigma) in peanut oil (P2144 Sigma) was injected i.p. in the F1 offspring at P30. TM doses of 3 mg and 9 mg/40g body weight and a vehicle control were utilized. Cre excision was detected as EGFP fluorescence in a wide variety of tissues, including FDL tendon, skin, cornea, muscle, intestine, and lung. The vehicle controls continued to express red fluorescence indicating a lack of Cre excision (data not shown). The data indicate that significant Cre-mediated recombination was detected 24 hours after a single 9 mg/40g body weight injection. We did a dose response analysis between 3 and 9mg/40g body weight with injections at days 1–3, followed by analysis at day 5 and 4.5 mg/40g body weight was determined to be optimum. The inducible mice (TM-*Dcn*$^{flox/flox}$/*Bgn*$^{flox/flox}$) were injected at day 21 and the FDL tendons were analyzed at day 45 (Supplemental Fig. S4). Expression of both decorin and biglycan was reduce to at or near background at 45 days (Supplemental Fig. S4A,B). Background was determine using the traditional decorin (*Dcn*$^{-/-}$) [21] and biglycan (*Bgn*$^{-/-}$) [22] knockout models as controls. Expression in the uninduced bitransgenic conditional mice Cre-*Dcn*$^{flox/flox}$/*Bgn*$^{flox/flox}$ was comparable to wild type controls. Protein levels for the decorin and biglycan protein cores were analyzed using immuno-blots at day 45, 23 days

after the final TM injection. The decorin and biglycan protein cores were significantly reduced compared to the wild type control (Supplemental Fig. S4C,D).

TM-induction protocol

Conditional compound decorin/biglycan knock out mice (I-*Dcn*$^{-/-}$/*Bgn*$^{-/-}$) and *Dcn*$^{+/+}$/*Bgn*$^{+/+}$ control (WT) mice (n=16/group) received three consecutive daily intraperitoneal tamoxifen injections (4.5mg/40g body weight) beginning at 120d. Wild type mice received identical tamoxifen injections. Mice were euthanized at 150d.

Histology

For histological analysis, the knee joint was removed by cutting through the femur and tibia at the time of sacrifice. The knee was flexed to 90°, placed into a cassette, fixed in formalin, and processed using standard paraffin histological techniques. Samples were embedded in paraffin and sections (7 μm) were stained with hematoxylin and eosin. Cell shape and cellularity were calculated using commercial software (Bioquant).

Gene and protein analysis

Real-time PCR—Patellar tendons were collected at the time of sacrifice and stored under liquid nitrogen. Frozen patellar tendons were cut into small pieces and total RNA was extracted using a micro RNeasy Kit (QIAGEN). Total RNA (4 ng per well) was subjected to reverse transcription using the High Capacity cDNA Reverse Transcription Kit (Applied Biosystems) and real-time PCR was performed with SYBR Green PCR master mix (Applied Biosystems) on a StepOnePlus Real Time PCR system (Applied Biosystems). The primer sequences were as follows: decorin forward primer, TGAGCTTCAACAGCATCACC, and decorin reverse primer, AAGTCATTTTGCCCAACTGC; biglycan forward primer, CTACGCCCTGGTCTTGGTAA, and biglycan reverse primer, ACTTTGCGGATACGGTTGTC; actin forward primer, AGATGACCCAGATCATGTTTGAGA and actin reverse primer, CACAGCCTGGATGGCTACGT. Each sample was run in duplicate (n=5/group) and data were analyzed using StepOne software c2.0 (Applied Biosystems). Actin was used as an internal control to standardize the amount of sample total RNA.

Immuno-fluorescence microscopy—For analyses of SLRP content, patellar tendons (n=3/group) collected and stored with those for PCR were thawed in ice-cold fixative containing 4% paraformaldehyde (EMS) and fixed at 4°C for 1 hour, processed through a sucrose gradient, embedded in OCT medium, frozen on dry ice and stored at −80°C. Frozen sections (5 μm thick) were cut with a Microm HM505E cryostat (Leica, Wetzlar, Germany). The slides were blocked with 5% donkey serum in PBS followed by rabbit anti-mouse decorin antibody (LF113; provided by Dr. Larry Fisher, National Institutes of Health, National Institute of Dental and Craniofacial Research, Bethesda, MD) or rabbit anti-mouse biglycan antibody (LF159; provided by Dr. Larry Fisher, National Institutes of Health, National Institute of Dental and Craniofacial Research, Bethesda, MD), both used at 1:200 dilution. The secondary antibody was Alexa Fluor 488-conjugated donkey anti-rabbit IgG (Molecular Probes) used at 1:200. Coverslips were mounted with Vectashield mounting solution containing DAPI (Vector Laboratories, Inc.) as a nuclear marker. Images were

captured with the use of a Leica CTR 5500 microscope and Leica DFC 340 FX camera. Identical conditions and set integration times were used to facilitate comparisons between samples.

Transmission Electron Microscopy

Samples designated for analysis of fibril structure were prepared for transmission electron microscopy. Patellar tendons from 4 different mice of each group was analyzed using transmission electron microscopy. The patellar tendons was fixed in situ using standard methods as previously described [16, 36, 37]. Add recent reference Post-staining with 2% aqueous uranyl acetate followed by 1% phosphotungstic acid, pH 3.2 was used for contrast enhancement. Cross sections through the midsubstance of the patellar tendons were examined at 80 kV using a JEOL 1400 transmission electron microscope. Images were digitally captured at an instrument magnification of 60,000× using an Orius widefield sidemount CCD camera at a resolution of 3648×2672. The digital images were masked and transferred to a RM Biometrics- Bioquant Image Analysis System (Memphis, TN) for analysis. Image magnification was calibrated using a line grating replica (PELCO®, Product No. 606). Fibril diameter analyses were done using images from the central portion of the tendon. All fibrils within a predetermined region of interest (ROI) on the digitized image were measured. Non-overlapping ROIs were placed based on fibril orientation (i.e., cross section) and absence of cells. Diameters were measured along the minor axis of the fibril. For measurement of fibril density, the total number of fibrils within the ROI was normalized for area.

Mechanical testing protocol

Patella-tendon-tibia complexes assigned to mechanical testing were dissected from knee as previously described. Tendon cross-sectional area was measured with custom laser device [38]. Tendons were stamped into a “dog-bone” shape using a 3D printed stage and 2mm biopsy punch. Verhoeff stain lines were applied at the tibial insertion, 1mm and 2mm from the insertion, and at the patella. The tibia was placed in a custom 3D printed pot and secured in PMMA. Custom fixtures were used to secure the pot for tensile testing.

Tendons were loaded in a 37°C 1× phosphate buffered saline bath in a tensile testing system (Instron 5848, Instron, Norwood, MA) integrated with an established cross-polarization light setup [39, 40]. This included a linear backlight (Dolan-Jenner, Boxborough, MA), rotating polarizer sheets offset by 90°(Edmund Optics, Barrington, NJ) on either side of the saline bath, and a digital camera (Basler, Exton, PA). The viscoelastic testing protocol consisted of preconditioning, stress relaxation, frequency sweeps (0.1, 1, 5, and 10 Hz) at 3%, 4%, and 5% strain, a return to zero displacement, a one minute hold, and finally a ramp to failure at a strain rate of 0.1%/s. At each stage of the testing protocol sets of 18 polarized light images were collected. Additional images were taken between segments at five second intervals and during the ramp to failure at 20 second intervals, as previously described [39]. Collagen fiber alignment, outputted as circular variance, was calculated from images collected during testing using a custom program (Matlab, Natick, MA), as previously described [41].

Failure load (N) was calculated from force-displacement data. Optical tracking data was used to compute midsubstance stiffness (N/mm) (Matlab, Natick, MA). Data normalized to cross-sectional area and tendon gauge length were used to determine Young's modulus (MPa). Dynamic modulus |E*| (the ratio of the amplitudes of the stress and strain sinusoids) and tan(δ) (the lag between stress and strain curves) were calculated at each strain-frequency combination. Unpaired Student's t-tests ($p<0.05$) were used to assess for significance differences in mechanical and structural properties between genotypes. Mann Whitney tests were used for non-normal data sets. One-way ANOVAs ($p<0.5/3$) with post-hoc Bonferroni corrections were also employed.

Supplementary Material

Refer to Web version on PubMed Central for supplementary material.

Acknowledgments

This work was supported by grants from NIH NIAMS AR068057, AR050950 and AR44745. The gene targeting, ES cell selection and blastocyst injection where done with the Genome Modification Facility at Harvard University. We would like to acknowledge the valuable technical assistance of Thomas Adams maintaining the mice and with fibril measurements.

Abbreviations

SLRP	small leucine rich proteoglycan
FDL	flexor digitorum longus
|E*|	dynamic modulus
TM	Tamoxifen
Cre	Cre recombinase
ROI	region of interest

References

1. Zhang G, Young BB, Ezura Y, Favata M, Soslowsky LJ, Chakravarti S, Birk DE. Development of tendon structure and function: Regulation of collagen fibrillogenesis. Journal of musculoskeletal & neuronal interactions. 2005; 5:5–21. [PubMed: 15788867]
2. Mienaltowski MJ, Birk DE. Structure, physiology, and biochemistry of collagens. Advances in experimental medicine and biology. 2014; 802:5–29. [PubMed: 24443018]
3. Zhang G, Ezura Y, Chervoneva I, Robinson PS, Beason DP, Carine ET, Soslowsky LJ, Iozzo RV, Birk DE. Decorin regulates assembly of collagen fibrils and acquisition of biomechanical properties during tendon development. Journal of cellular biochemistry. 2006; 98:1436–1449. [PubMed: 16518859]
4. Ameye L, Young MF. Mice deficient in small leucine-rich proteoglycans: Novel in vivo models for osteoporosis, osteoarthritis, ehlers-danlos syndrome, muscular dystrophy, and corneal diseases. Glycobiology. 2002; 12:107R–116R.
5. Ezura Y, Chakravarti S, Oldberg A, Chervoneva I, Birk DE. Differential expression of lumican and fibromodulin regulate collagen fibrillogenesis in developing mouse tendons. The Journal of cell biology. 2000; 151:779–788. [PubMed: 11076963]

6. Chakravarti S, Zhang G, Chervoneva I, Roberts L, Birk DE. Collagen fibril assembly during postnatal development and dysfunctional regulation in the lumican-deficient murine cornea. Developmental dynamics : an official publication of the American Association of Anatomists. 2006; 235:2493–2506. [PubMed: 16786597]
7. Ameye L, Aria D, Jepsen K, Oldberg A, Xu T, Young MF. Abnormal collagen fibrils in tendons of biglycan/fibromodulin-deficient mice lead to gait impairment, ectopic ossification, and osteoarthritis. FASEB journal : official publication of the Federation of American Societies for Experimental Biology. 2002; 16:673–680. [PubMed: 11978731]
8. Corsi A, Xu T, Chen XD, Boyde A, Liang J, Mankani M, Sommer B, Iozzo RV, Eichstetter I, Robey PG, Bianco P, Young MF. Phenotypic effects of biglycan deficiency are linked to collagen fibril abnormalities, are synergized by decorin deficiency, and mimic ehlers-danlos-like changes in bone and other connective tissues. Journal of bone and mineral research : the official journal of the American Society for Bone and Mineral Research. 2002; 17:1180–1189.
9. Svensson L, Aszodi A, Reinholt FP, Fassler R, Heinegard D, Oldberg A. Fibromodulin-null mice have abnormal collagen fibrils, tissue organization, and altered lumican deposition in tendon. The Journal of biological chemistry. 1999; 274:9636–9647. [PubMed: 10092650]
10. Chen S, Birk DE. The regulatory roles of small leucine-rich proteoglycans in extracellular matrix assembly. The FEBS journal. 2013; 280:2120–2137. [PubMed: 23331954]
11. Schaefer L, Iozzo RV. Biological functions of the small leucine-rich proteoglycans: From genetics to signal transduction. The Journal of biological chemistry. 2008; 283:21305–21309. [PubMed: 18463092]
12. Iozzo RV, Schaefer L. Proteoglycan form and function: A comprehensive nomenclature of proteoglycans. Matrix biology : journal of the International Society for Matrix Biology. 2015; 42:11–55. [PubMed: 25701227]
13. Schonherr E, Hausser H, Beavan L, Kresse H. Decorin-type i collagen interaction. Presence of separate core protein-binding domains. The Journal of biological chemistry. 1995; 270:8877–8883. [PubMed: 7721795]
14. Schonherr E, Witsch-Prehm P, Harrach B, Robenek H, Rauterberg J, Kresse H. Interaction of biglycan with type i collagen. The Journal of biological chemistry. 1995; 270:2776–2783. [PubMed: 7852349]
15. Gubbiotti MA, Vallet SD, Ricard-Blum S, Iozzo RV. Decorin interacting network: A comprehensive analysis of decorin-binding partners and their versatile functions. Matrix biology : journal of the International Society for Matrix Biology. 2016; 55:7–21. [PubMed: 27693454]
16. Dunkman AA, Buckley MR, Mienaltowski MJ, Adams SM, Thomas SJ, Satchell L, Kumar A, Pathmanathan L, Beason DP, Iozzo RV, Birk DE, Soslowsky LJ. Decorin expression is important for age-related changes in tendon structure and mechanical properties. Matrix biology : journal of the International Society for Matrix Biology. 2013; 32:3–13. [PubMed: 23178232]
17. Elliott DM, Robinson PS, Gimbel JA, Sarver JJ, Abboud JA, Iozzo RV, Soslowsky LJ. Effect of altered matrix proteins on quasilinear viscoelastic properties in transgenic mouse tail tendons. Annals of biomedical engineering. 2003; 31:599–605. [PubMed: 12757203]
18. Robinson PS, Lin TW, Jawad AF, Iozzo RV, Soslowsky LJ. Investigating tendon fascicle structure-function relationships in a transgenic-age mouse model using multiple regression models. Annals of biomedical engineering. 2004; 32:924–931. [PubMed: 15298430]
19. Dourte LM, Pathmanathan L, Jawad AF, Iozzo RV, Mienaltowski MJ, Birk DE, Soslowsky LJ. Influence of decorin on the mechanical, compositional, and structural properties of the mouse patellar tendon. J Biomech Eng. 2012; 134:031005. [PubMed: 22482685]
20. Dourte LM, Pathmanathan L, Mienaltowski MJ, Jawad AF, Birk DE, Soslowsky LJ. Mechanical, compositional, and structural properties of the mouse patellar tendon with changes in biglycan gene expression. J Orthop Res. 2013; 31:1430–1437. [PubMed: 23592048]
21. Danielson KG, Baribault H, Holmes DF, Graham H, Kadler KE, Iozzo RV. Targeted disruption of decorin leads to abnormal collagen fibril morphology and skin fragility. The Journal of cell biology. 1997; 136:729–743. [PubMed: 9024701]
22. Xu T, Bianco P, Fisher LW, Longenecker G, Smith E, Goldstein S, Bonadio J, Boskey A, Heegaard AM, Sommer B, Satomura K, Dominguez P, Zhao C, Kulkarni AB, Robey PG, Young MF.

Targeted disruption of the biglycan gene leads to an osteoporosis-like phenotype in mice. Nature genetics. 1998; 20:78–82. [PubMed: 9731537]

23. Zhang G, Chen S, Goldoni S, Calder BW, Simpson HC, Owens RT, McQuillan DJ, Young MF, Iozzo RV, Birk DE. Genetic evidence for the coordinated regulation of collagen fibrillogenesis in the cornea by decorin and biglycan. The Journal of biological chemistry. 2009; 284:8888–8897. [PubMed: 19136671]
24. Beavan LA, Quentin-Hoffmann E, Schonherr E, Snigula F, Leroy JG, Kresse H. Deficient expression of decorin in infantile progeroid patients. The Journal of biological chemistry. 1993; 268:9856–9862. [PubMed: 8486665]
25. Wadhwa S, Bi Y, Ortiz AT, Embree MC, Kilts T, Iozzo R, Opperman LA, Young MF. Impaired posterior frontal sutural fusion in the biglycan/decorin double deficient mice. Bone. 2007; 40:861–866. [PubMed: 17188951]
26. Young MF, Bi Y, Ameye L, Chen XD. Biglycan knockout mice: New models for musculoskeletal diseases. Glycoconjugate journal. 2002; 19:257–262. [PubMed: 12975603]
27. Iozzo, RV., Goldoni, S., Berendsen, A., Young, M. Small leucine-rich proteoglycans. In: Mecham, RP., editor. The extracellular matrix: An overview. biology of extracellular matrix; Springer-Verlag Berlin Heidelberg: 2011. p. 197-232.
28. Moreth K, Iozzo RV, Schaefer L. Small leucine-rich proteoglycans orchestrate receptor crosstalk during inflammation. Cell Cycle. 2012; 11:2084–2091. [PubMed: 22580469]
29. Schaefer L, Tredup C, Gubbiotti MA, Iozzo RV. Proteoglycan neofunctions: Regulation of inflammation and autophagy in cancer biology. The FEBS journal. 2017; 284:10–26. [PubMed: 27860287]
30. Young MF, Fallon JR. Biglycan: A promising new therapeutic for neuromuscular and musculoskeletal diseases. Current opinion in genetics & development. 2012; 22:398–400. [PubMed: 22841370]
31. Redaelli A, Vesentini S, Soncini M, Vena P, Mantero S, Montevecchi FM. Possible role of decorin glycosaminoglycans in fibril to fibril force transfer in relative mature tendons--a computational study from molecular to microstructural level. Journal of biomechanics. 2003; 36:1555–1569. [PubMed: 14499303]
32. Wu Z, Aron AW, Macksoud EE, Iozzo RV, Hai CM, Lechner BE. Uterine dysfunction in biglycan and decorin deficient mice leads to dystocia during parturition. PloS one. 2012; 7:e29627. [PubMed: 22253749]
33. Connizzo BK, Sarver JJ, Han L, Soslowsky LJ. In situ fibril stretch and sliding is locationdependent in mouse supraspinatus tendons. Journal of biomechanics. 2014; 47:3794–3798. [PubMed: 25468300]
34. Connizzo BK, Yannascoli SM, Soslowsky LJ. Structure-function relationships of postnatal tendon development: A parallel to healing. Matrix biology : journal of the International Society for Matrix Biology. 2013; 32:106–116. [PubMed: 23357642]
35. Sun M, Chen S, Adams SM, Florer JB, Liu H, Kao WW, Wenstrup RJ, Birk DE. Collagen v is a dominant regulator of collagen fibrillogenesis: Dysfunctional regulation of structure and function in a corneal-stroma-specific col5a1-null mouse model. J Cell Sci. 2011; 124:4096–4105. [PubMed: 22159420]
36. Birk DE, Trelstad RL. Extracellular compartments in tendon morphogenesis: Collagen fibril, bundle, and macroaggregate formation. The Journal of cell biology. 1986; 103:231–240. [PubMed: 3722266]
37. Birk DE, Zycband EI, Woodruff S, Winkelmann DA, Trelstad RL. Collagen fibrillogenesis in situ: Fibril segments become long fibrils as the developing tendon matures. Developmental dynamics : an official publication of the American Association of Anatomists. 1997; 208:291–298. [PubMed: 9056634]
38. Favata M, Beredjiklian PK, Zgonis MH, Beason DP, Crombleholme TM, Jawad AF, Soslowsky LJ. Regenerative properties of fetal sheep tendon are not adversely affected by transplantation into an adult environment. J Orthop Res. 2006; 24:2124–2132. [PubMed: 16944473]

39. Lake SP, Miller KS, Elliott DM, Soslowsky LJ. Effect of fiber distribution and realignment on the nonlinear and inhomogeneous mechanical properties of human supraspinatus tendon under longitudinal tensile loading. J Orthop Res. 2009; 27:1596–1602. [PubMed: 19544524]

40. Connizzo BK, Han L, Birk DE, Soslowsky LJ. Collagen v-heterozygous and -null supraspinatus tendons exhibit altered dynamic mechanical behaviour at multiple hierarchical scales. Interface focus. 2016; 6:20150043. [PubMed: 26855746]

41. Miller KS, Connizzo BK, Feeney E, Soslowsky LJ. Characterizing local collagen fiber realignment and crimp behavior throughout mechanical testing in a mature mouse supraspinatus tendon model. J Biomech Eng. 2012; 45:2061–2065.

Highlights

- Inducible mouse models were created and used to determine the effects of decorin and biglycan expression on tendon homeostasis.
- Acute ablation of both decorin and biglycan expression in the mature tendon resulted in alterations in collagen fibril structure.
- Both decorin and biglycan are required for the maintenance of mechanical properties in the mature tendon.
- Collagen fiber realignment after loading is dependent on decorin and biglycan expression in the mature tendon.

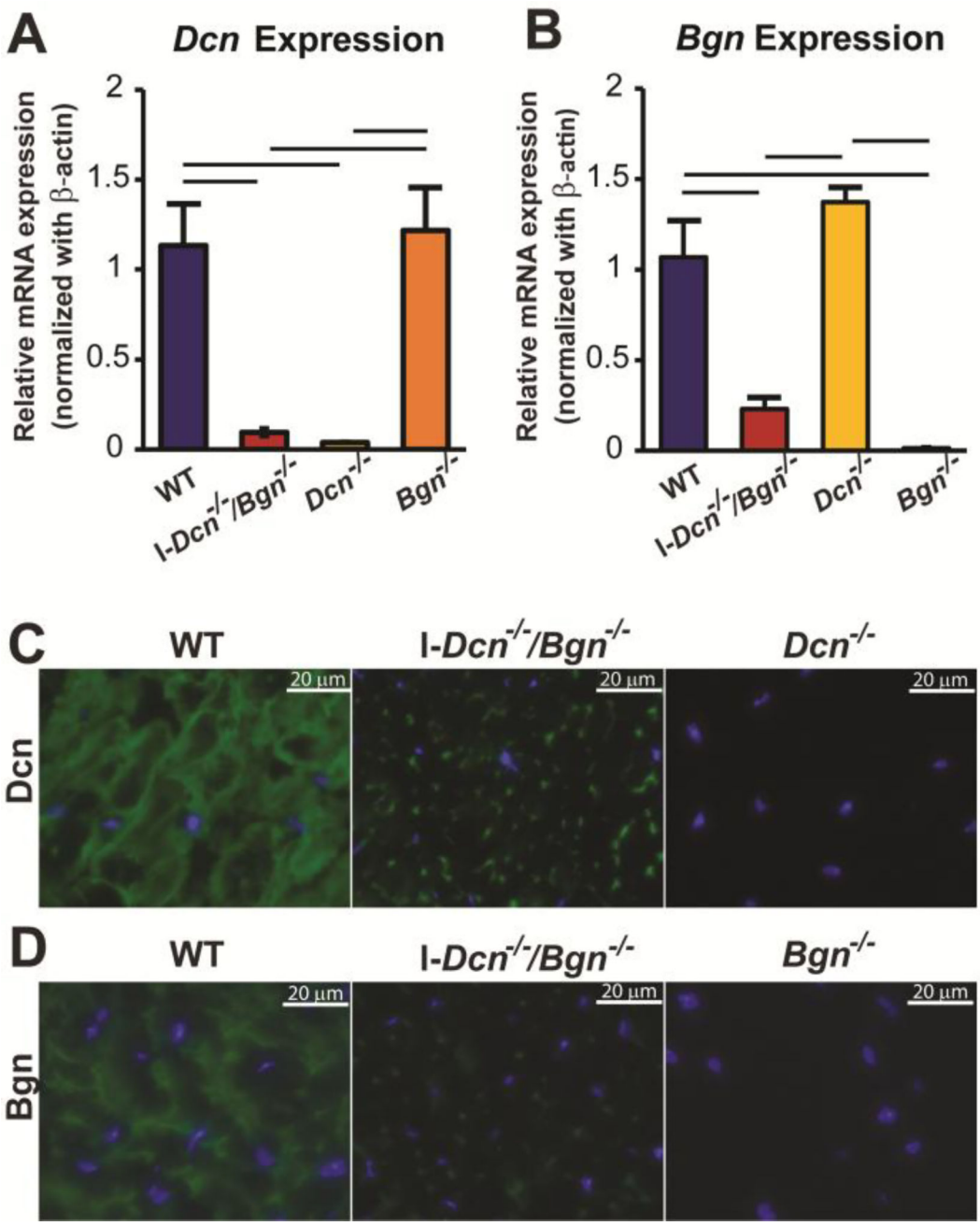

Fig. 1. Knockdown of decorin and biglycan expression in I-*Dcn*$^{-/-}$/*Bgn*$^{-/-}$ patellar tendons

Characterization of decorin **(A)** and biglycan **(B)** expression in I-*Dcn*$^{-/-}$/*Bgn*$^{-/-}$ patellar tendons 30 days after Induction of Cre. Decorin and biglycan expression were reduced to background in I-*Dcn*$^{-/-}$/*Bgn*$^{-/-}$ tendons compared to TM treated wild type controls (WT). The background was established using traditional decorin (*Dcn*$^{-/-}$) and biglycan (*Bgn*$^{-/-}$) knockout mice. Real-time PCR, n=5 tendons from 5 different mice. Bars indicate statistical significance ($p<0.05$). Decorin **(C)** and biglycan **(D)** protein in patellar tendons 30 days after knockout of *Dcn* and *Bgn* expression. Decorin (Dcn) and biglycan (Bgn) reactivity was substantially reduced in I-*Dcn*$^{-/-}$/*Bgn*$^{-/-}$ tendons, but above background as determined

using decorin ($Dcn^{-/-}$) and biglycan ($Bgn^{-/-}$) knockout mice. Representative immunofluorescence images taken from patellar tendons from different mice (n=3). Dcn and Bgn, green. Nuclei are visualized using DAPI. Day 120 female mice received 3 daily injections of TM and tendons were analyzed at day 150.

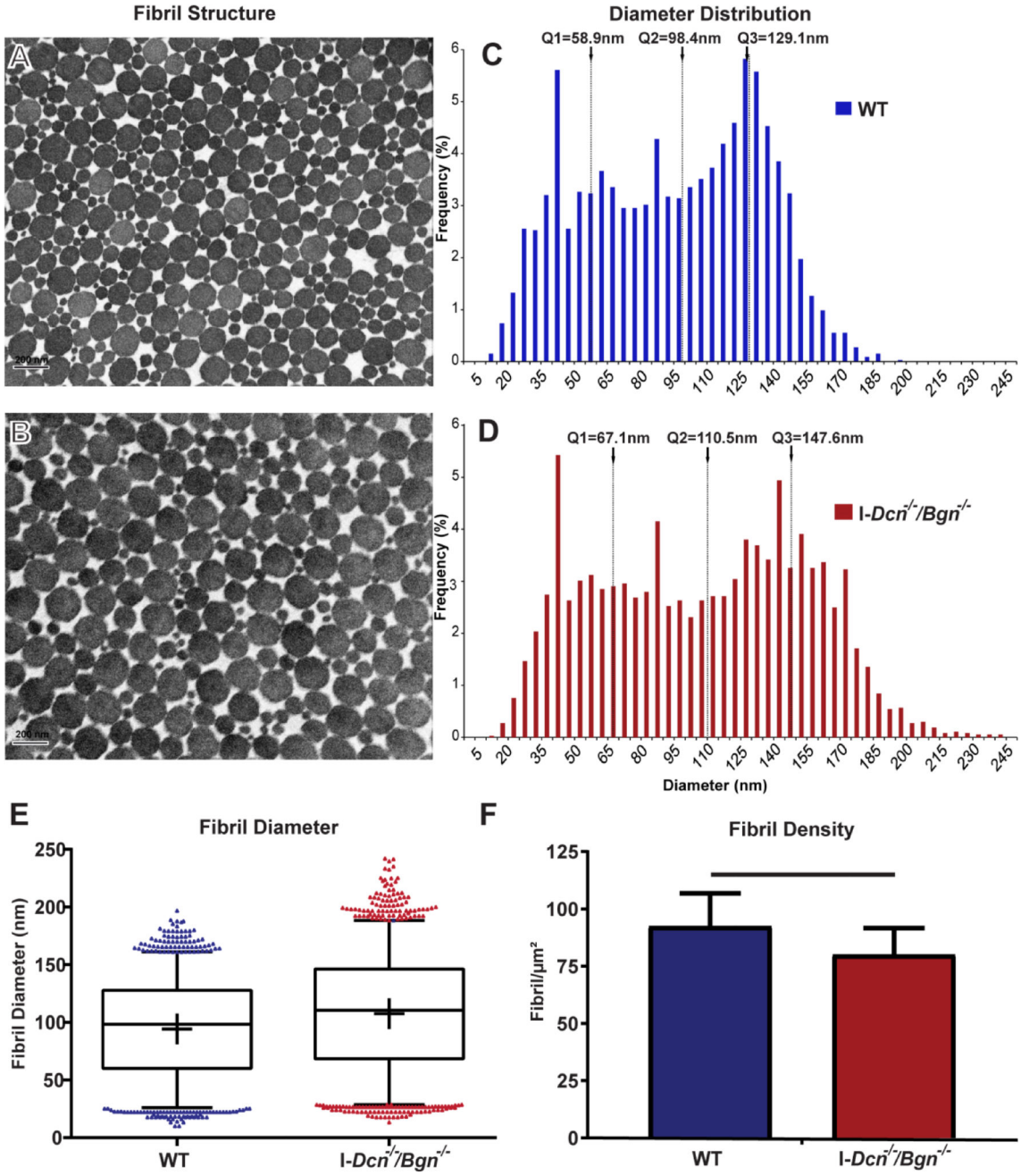

Fig. 2. Decorin and biglycan expression in mature tendons is required to maintain collagen fibril structure

Transmission electron micrographs of wild type **(A)** and I-$Dcn^{-/-}/Bgn^{-/-}$ **(B)** patellar tendons showing collagen fibrils. Both wild type (WT) and I-$Dcn^{-/-}/Bgn^{-/-}$ fibrils have comparable cross-sectional contours. (**C,D**) Fibril diameter distributions demonstrated a shift towards larger diameter fibrils with increased heterogeneity in the I-$Dcn^{-/-}/Bgn^{-/-}$ compared with WT tendons. **(E)** Analysis of fibril diameter distributions in mature tendons 30 days after knockout of decorin and biglycan. Fibril diameters in the I-$Dcn^{-/-}/Bgn^{-/-}$ tendons were larger with a broader distribution than in the WT controls with an increase in

the number of large diameter outliers. Boxplots span data between the 2nd and 98th percentile. Data points outside this range are shown with individual markers. **(F)** Fibril density was significantly lower in I-*Dcn*$^{-/-}$/*Bgn*$^{-/-}$ tendons compared with the wild type controls ($p<0.005$). The means ± sd (n) were 79.9 ± 11.6 (55) fibrils/μm^2 versus 92.2 ± 14.3 (42) fibrils/μm^2, for I-*Dcn*$^{-/-}$/*Bgn*$^{-/-}$ and WT tendons. Mature female mice were injected with TM at day 120 and patellar tendons analyzed at day 150. n=4 mice/group.

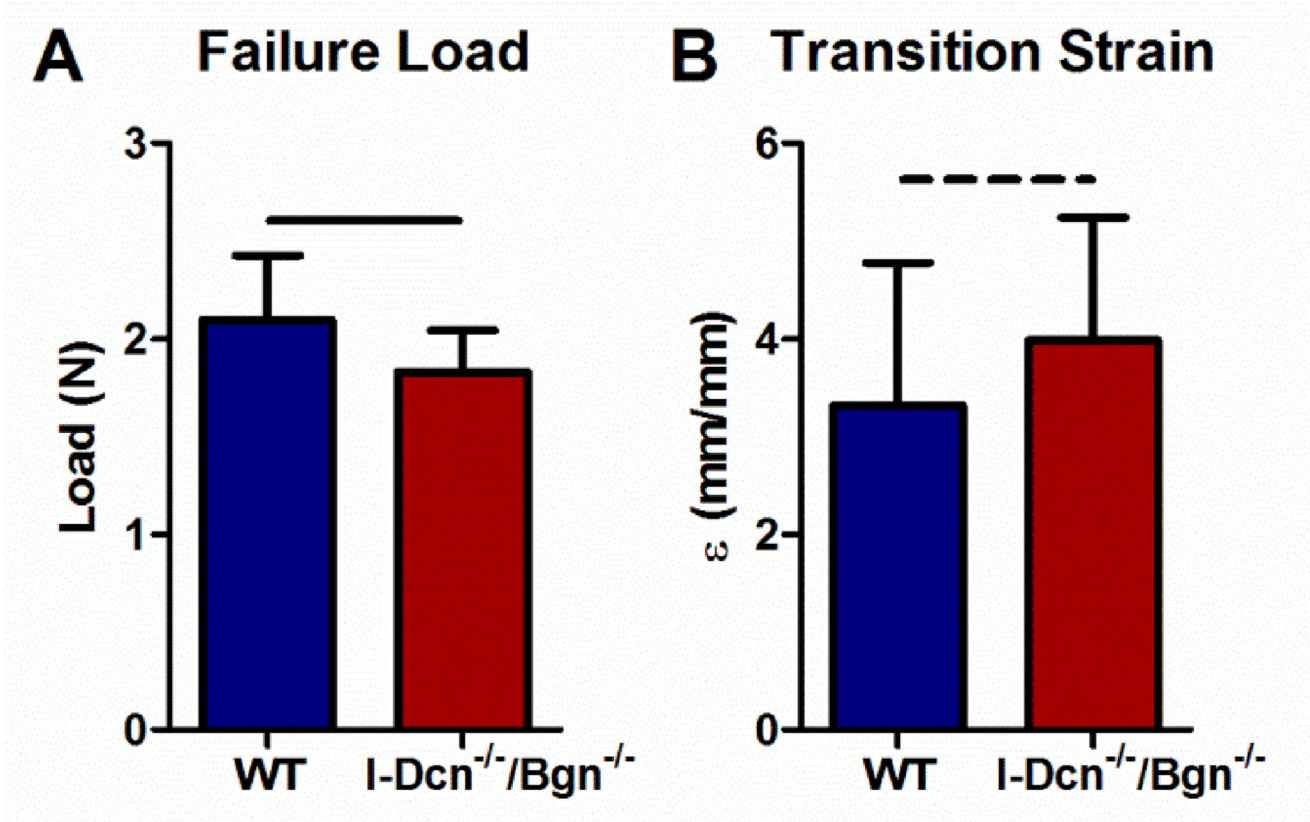

Fig. 3. Absence of decorin and biglycan expression in mature tendons reduces failure load and increases transition strain

I-*Dcn*$^{-/-}$/*Bgn*$^{-/-}$ tendons failed at lower loads than controls **(A)** and had increased transition strain **(B)** compared to wild type (WT) tendons indicating decreased tensile strength in ramp to failure tests. Patellar tendons from female mice were analyzed at day 150, n=16 mice/group.

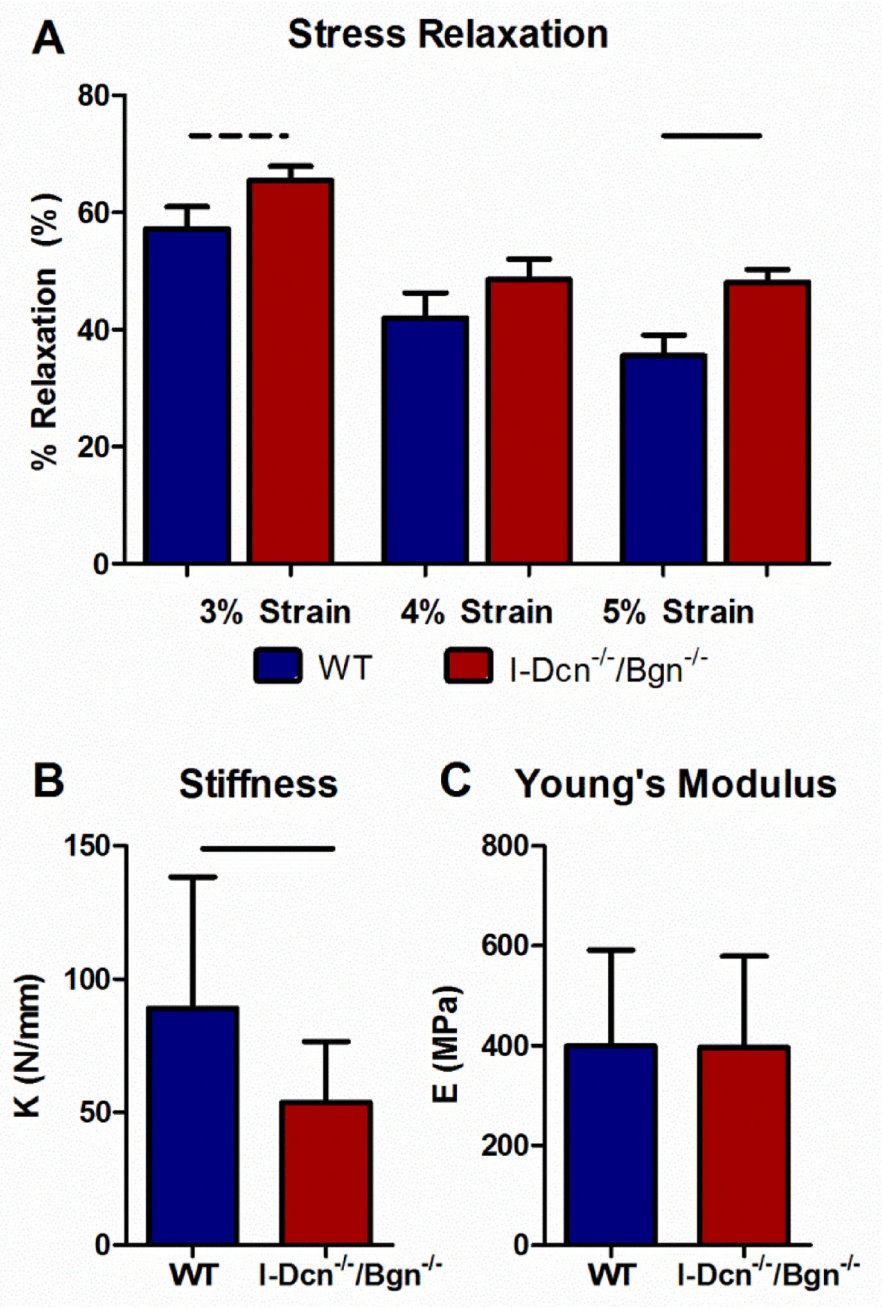

Fig. 4. Tendon stiffness decreases in the absence of decorin and biglycan expression

I-*Dcn*$^{-/-}$/*Bgn*$^{-/-}$ patellar tendons exhibited increased percent relaxation **(A)** at 3% strain (trend) and 5% strain compared to wild type tendons. I-*Dcn*$^{-/-}$/*Bgn*$^{-/-}$ tendons were stiffer **(B)** than wild type tendons, but Young's modulus was similar in both groups **(C)**. Patellar tendons from female mice were analyzed at day 150, n=16 mice/group.

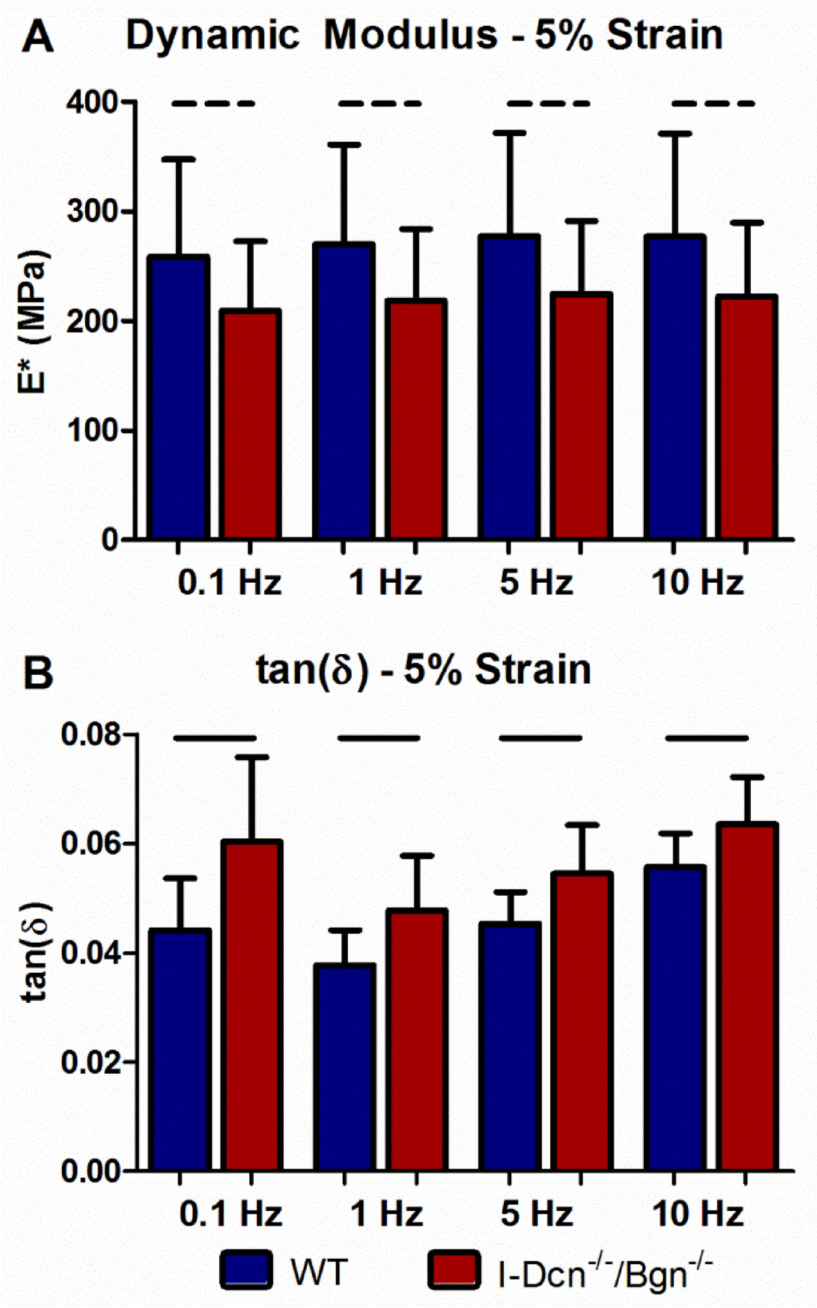

Fig. 5. Dynamic modulus decreases and tan(δ) increases in the absence of decorin and biglycan expression

I-*Dcn*$^{-/-}$/*Bgn*$^{-/-}$ tendons had decreased dynamic modulus (trend) indicating a decreased capacity to transfer force without continued decorin and biglycan expression. A significant increase in tan(δ) at 3% (not shown), 4% (not shown), and 5% strain was observed in I-*Dcn*$^{-/-}$/*Bgn*$^{-/-}$ tendons compared to WT controls. The increase in tan(δ) in the absence of decorin and biglycan expression indicates an altered ability to dissipate stored force during cyclic loading. Patellar tendons from female mice were analyzed at day 150, n=16 mice/group.

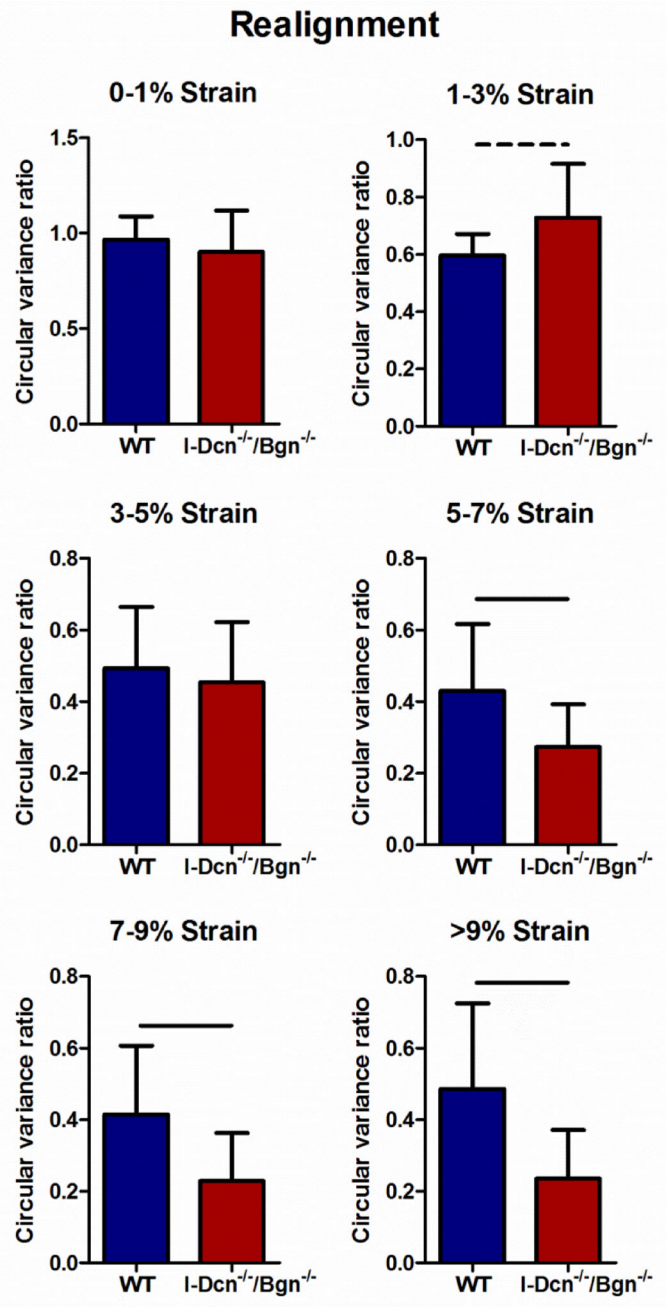

Fig. 6. Fiber realignment increased at linear strains in the mature tendon in the absence of decorin and biglycan expression

I-*Dcn*$^{-/-}$/*Bgn*$^{-/-}$ tendons exhibited increased realignment at linear strain levels compared to WT controls. The decreased circular variance ratio in I-*Dcn*$^{-/-}$/*Bgn*$^{-/-}$ tendons indicates an increase in collagen fiber alignment during tendon loading and a role for decorin/biglycan in this process. Patellar tendons from female mice were analyzed at day 150, n=16 mice/group.

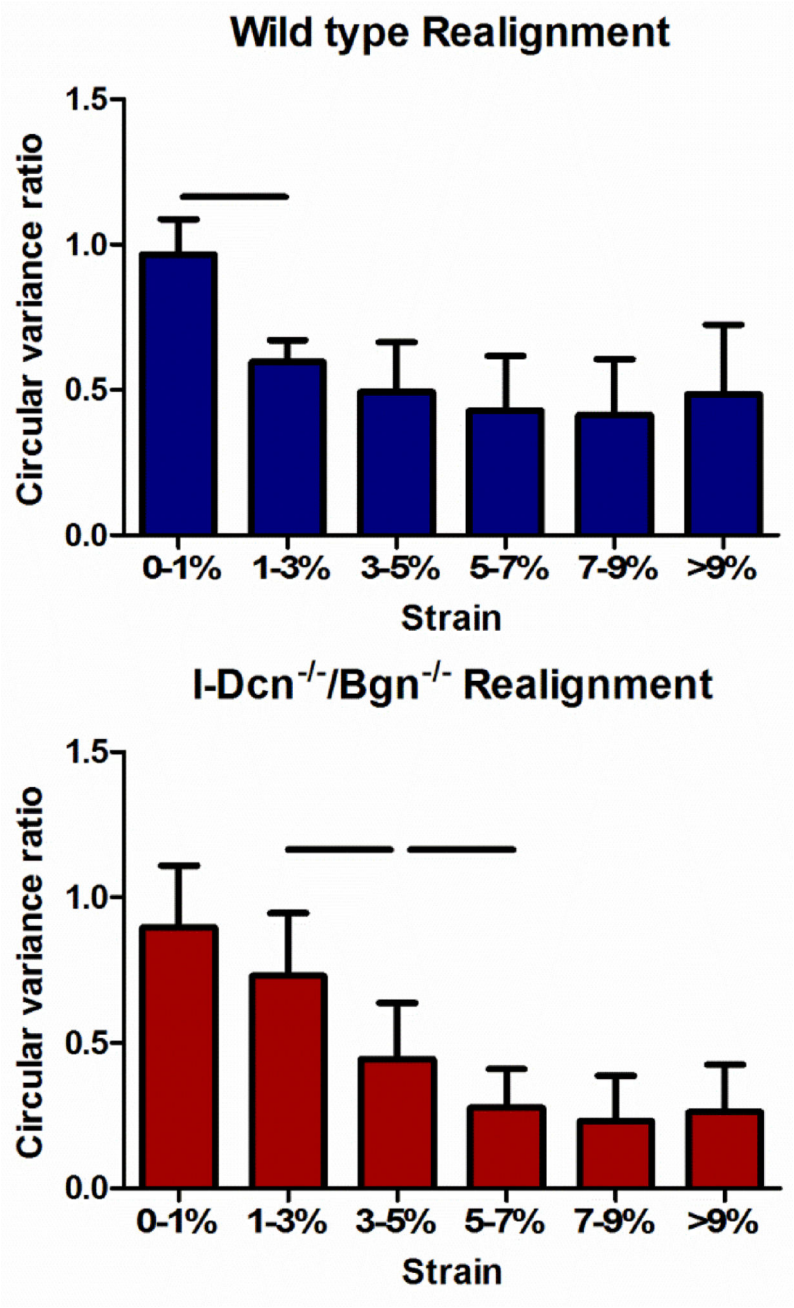

Fig. 7. Fiber realignment was delayed in the absence of decorin and biglycan expression

I-*Dcn*$^{-/-}$/*Bgn*$^{-/-}$ tendon midsubstance realigned later and more slowly compared to wild type tendons. Patellar tendons from female mice were analyzed at day 150, n=16 mice/group.